Mithlesh Sharma, Deepak Kumar Goyal, Gagandeep Kaushal

Numerical Simulation and Characterization of Slurry Erosion of HVOF Coated Surfaces by Using Failure Analysis Approach

Mithlesh Sharma[1], Deepak kumar Goyal[2], Gagandeep Kaushal[3]
[1] Research Scholar, IKGPTU, Kapurthala, Punjab
[2] Assistant Prof., IKGPTU Main Campus, Kapurthala, Punjab
[3] Assistant Prof., YCOE, Punjabi Univ. Campus, Talwandi Sabo, Punjab

Abstract

In present study an attempt was made to numerically simulate the slurry erosion process using material failure modelof progressive damage slurry erosion process was numerically simulated by using material failure model (MFM) of progressive damage instigation and promulgation for the impingement of solid and liquid particles on the solid surfaces. To simulate this problem Finite element analysis based three dimensional Abaqus Explicit software has been used. The mixture which comprises of solid and liquid particles known as slurry, when impinged upon the surface of the component surface leads to impingement of solid and liquid particles on the solid surface which leads to dreadful conditions on the surface known as slurry erosion. The proposed model uses the FEA concepts of adaptive meshing, strain-dependent damage initiation Criteria, a general contact algorithm, damage propagation, enhanced hourglass section control and multiple particle Impingements to study the slurry erosion process. For the purpose of experimental validation and due to the availability of material properties, surface coatings of a powder on steel are deposited by the HVOF Coating process. The slurry erosion tests are performed on these depositions using the abrasive slurry at different impingement angles. The tests are made in an Impact test erosion rig. From these tests, the material removal rate (MRR) values and depth of penetration including the profiles of the craters are computed as a function of the slurry jet impingement angles. The numerically computed results are compared with the experimental results and are shown to be in good agreement.

Key Words: High Velocity Oxy Fuel Coating Process (HVOF), Finite element analysis, Adaptive meshing, Material failure analysis, Slurry erosion.

1. INTRODUCTION

In this developing world, there is a growing need for industrialization. To fulfill this need industry requires energy sources to cater its demand. In particular demand of electrical energy is increasing rapidly day by day [1]. Hydropower being a renewable source of energy has fascinated the attention of researchers worldwide for harnessing its potential to fulfill the increasing demand of energy requirement [2-4]. With increasing dependency on hydropower, more burdens have been laid on hydroelectric power stations which resulted in extensive usage of available hydro power resources. To cater the demand, hydroelectric power plants are running under unfavorable conditions such as under high silt content. High silt content in the water leads to extensive material removal from various components of hydraulic machinery. In particular, various components associated with hydro machinery such as turbine blades, labyrinth seals and guide vanes are on the extent of maximum damage by abrasive particles [2]. Slurry erosion in hydro power plant is a major concern, particularly in the hydro power plant

which are feeded from tributaries originating from Himalayan region, where during rainy season silt content increases in the water (up to 10000 ppm) passing through the turbines [3]. Hydro power plants which are worstly impacted by slurry erosion damage in India are Chameri, Maneri Bhali–I, Nathpa Jhakri, Koteshwar and Dehar where amount of damage is very high and it needs break down after every one or two monsoons. This has resulted in huge monetary loss, reduced effectiveness, forced outages and repair to the hydro power station situated in the Himalayan region [5]. Therefore it is essential to identify the erosion mechanism of material which causes degradation of material and measures by which it can be pr0evented. Researchers have reported that slurry erosion of a material depend upon various process parameters such as impacting velocity of jet, impact angle, morphology of erodent particle, mechanical and micro structural properties of the targeting component and erodent particle(1). It is very difficult to investigate the influence on all these parameters on slurry erosion process by experimentation alone. To overcome such restriction researchers had revealed a new technique known as Numerical simulation. Extensive experimentation which causes wastage of time and money will be substituted by validated numerical simulations results. These simulated results have potential in various applications such as Marine industry, Power generation, oil industry, Pumps, Valves, piping industry etc. Various researchers [2–7] had worked on the development of model to study the slurry erosion phenomenon by utilizing different modeling technique and simulations mechanism. In very beginning of this concept of erosion process modeling, Finnie had established a model to investigate the impingement behavior of single particle on to the metals [2] and solid surfaces [3], Bitter had proposed erosion models [4–5] which are based on plasticity behavior, element deletion, hertizan contact theory and energy balance equation approach. Hutchings [6] proposed a model which considers plastic strain approach for investigating the exposure of spherical particles on the target surface at normal impact. Furthermore Hashish [7] proposed a advanced finnie's model by including the effect of particle morphology on to the erosion process. Researchers (8-15) are continuously working on numerical modeling of the slurry erosion process using variety of Finite element analysis software. Woytowitz et al. [8] investigated erosion process using Nonlinear Finite element analysis from solid mechanics view point. Chen et al. [9] presented a computational mean particle erosion model and had reasonable agreement with experimental results. Elalem et al. [10] developed a Micro-Scale Dynamic Model (MSDM) for simulating the wear behavior of materials on the microscales. Shimizu et al. [11] used Tabor's theory and Finite Element Method (FEM) for modeling the surface damage caused by the impact of solid particles in a gas or liquid stream. Chen et al. [12] used a MSDM for simulating the solid particle erosion process. Papini et al. [13] developed a computer algorithm model to account for the interference action between the rebounding and incident streams in erosion testing. Griffin et al. [14] developed a 3D FEA model for solid particle erosion using the element removal method. Eltobgy et al. [15] modeled the 3D erosion process and considered multiple particle interaction. This article focuses on applying the failure analysis methodology to simulate the erosion process using commercially available ABAQUS/Explicit analysis software.

In this present investigation AISI 304 steel has been chosen for the erosion studies. To enhance the erosion resistance of the above said material, WC-10Co-4Cr coating layer with thickness of 220-250μm has been developed. Experimental investigation was carried out on the above said material. Further an attempt has been made to develop a numerical model which will be able to

investigate the slurry erosion process. For development of Numerical model Finite Element analysis software named as Abaqus has been used. Element deletion mesh along with Johnson Cook model has been used. The damage initiation and propagation of the solid surfaces is modeled for multiple particles. The numerical simulation results of solid surfaces are validated with an experiment   and the experimental results are in reasonable agreement with the simulations.

2. EXPERIMENTAL PROCESS DETAILS

2.1 Details of Materials

2.1.1   Base Materials

In present investigation ManeriBhali stage -1 has been chosen for study. It has been reported that high silt particles during monsoon season damage the various components of Hydro power plant such as Runner, blade, Liner, casing etc. Cut section from the hydro turbine component has been taken. Spectroscopy composition test of the cut section has been carried out as shown in Table 1. It has been revealed that the material taken from hydro power plants conforms the standard of ASTM 240/ AISI 304 Steel.

Table 1. Chemical composition of the AISI304 grade of ASTM A240 stainless steel (wt. %)

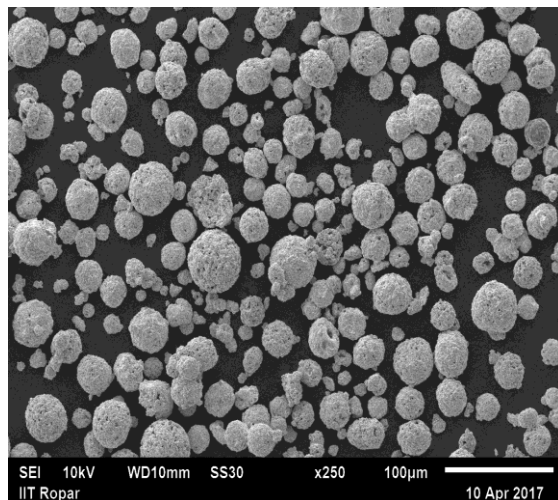| Grade	Cmax	Si	Mn	P	S	Ni	Cr	Fe
AISI 304	0.02	0.475	1.85	.0440	0.0302	8	18	Balance

2.1.2 Coating powder

In present investigation HVOF coating has been deposited on to the surface of AISI304 Steel. HVOF facility is available at Metalizing Equipment Private limited, Jodhpur, India. Researcher (1-7) revealed that HVOF coating produces dense structured, harder, tougher, higher bond strength. These advantages of HVOF led to development of layer on to the AISI304 Stainless steel. WC-10Co-4Cr powder was developed on to the specimen of AISI 304 Stainless steel by using HVOF Thermal spray process. The chemical composition of this powder is shown in Table 2. Powder morphology of the particle revealed that powder particles are of -45 +15µm size with irregular shape as shown in Figure 1. The morphology of the powder is shown in Figure 1. From the figure it was depicted that powder particle comprises of spheroidal and nodular particles

Table 2 Details of the coating powder used in the current investigation

Powder	Make	Morphology	Particle shape	Particle size
WC-10Co-4Cr	Hunter	Agglomerated sintered	Irregular/ Sub angular	–45 +15 µm

---

Mithlesh Sharma, Deepak Kumar Goyal, Gagandeep Kaushal

| 1. Flow control valve |
| 2. Electromagnetic flow meter |
| 3. Specimen container |
| 4. Centrifugal pump |
| 5. Slurry tank |

Fig.-3 Schematic View of Jet Erosion Tester

2.4 Erosion testing

Slurry erosion testing of sample was carried out to determine the behavior of material under the erosive conditions. These tests were carried out using impact test rig available at IET Bhaddal, Ropar, as shown in Figure 4. The test rig comprises a mud pump, conical tank, nozzle, specimen holder, valves and flow meter. The purpose of using mud pump is to lift the slurry in the pipe and to circulate it into the pipe. With the help of flow meter, flow rate of slurry is measured.. Flow rate of slurry is controlled by the help of flow control valve. Specimen is placed in a specimen container and slurry is impacted at different impact angle. Slurry is re-circulated during test. During test the temperature of slurry increase to a certain level and thereafter remains constant, which is due to mechanical action of pump. The flow rate of the slurry is controlled with help of main valve and bypass regulator valve between delivery side and nozzle. A fine wire screen mesh is provided in the bottom of the tank to avoid the object from falling into the tank and got struck inside the pipeline.

Slurry flowing through the pump at high pressure is converted into high velocity stream while passing through the converging section of the nozzle which is 125mm long and having diameter of 8 mm. the standoff distance between the nozzle and specimen can be varied from 25mm to 90mm. After striking the specimen slurry falls back into the tank, as the holder is located on the top of tank enclosed in a casing made of steel angle and fitted with fiber sheet, to facilitate the removal and clamping of the specimen. The electronic magnetic flow meter (Elmag-200M) is placed in between control valve and nozzle as shown in figure 3 consisting digital display. This flow meter works on the principal of faradays law of induction which states that when a conductive fluid passes through a magnetic field, voltage is induced which is directly proportional to the flowing velocity of fluid. For all experiments the slurry concentration of 5000ppm were taken. Experiments were carried out at a three levels of impingement velocity of 25 m/s, 50m/s and 75m/s at 90^0 impingement angles. Slurry erosion testing of the sample was carried out for the time duration of 120 mins. The test samples were cleaned with the help of acetone prior to testing and after testing. Sample weight prior to testing and after testing was carried out using weight balance with a least count of 0.001mg. The material removal rate is calculated by mass loss per unit time and is calculated using the following formula:

Material Removal Rate (MRR) = $(W_i - W_{f)}$ / (Unit Amount of Time)

Where W_i is the initial mass of each sample and W_f is the final mass after erosion testing.

2.5 Characterization

The characterization of the substrate and coated surface was carried out by using Scanning Electron microscopy. SEM testing was carried out to investigate the surface topography of the substrate and HVOF coated samples. SEM was carried out on JSM-II, JEOL at NITTTR, Chandigarh, India. It is used to observe the surfaces and sub surfaces of the eroded samples after testing to evaluate the behavior of sample under erosive conditions. With the help of characterization evaluation regards to damage initiation and mechanism by which it had propagated will be evaluated. Further characterization of the damaged sample was carried out by using Mitutoyo Roughness tester SJ-301 available at IET Bhaddal, Ropar, India. With the help of this tester depth of craters which are formed by the penetration of the erodent was measured. Least count of roughness tester is .001μm.

3. FINITE ELEMENT MODEL BASED ON DAMAGE INITIATION AND PROPAGATION

1. Finite Element Model Formulation

Finite element modeling was carried out with a focus on investigation of the damage caused by the impacting erodent particles on the target surface.

It was observed during experimentation that large deformation was taken place on the target surface in erosion process. For simulating the erosion process commercially available three dimensional FEA Abaqus explicit software with the capability of damage instigation and promulgation. For modeling the erosion process general contact algorithm is used with node to node surfaces along with mesh deletion element was used. A general contact algorithm was choosen between the solid particles and the target using normal behavior of contact by taking penalty method is used by the ABAQUS/ Explicit solver. The advantage of using Explicit solver is that it can reduce the time used for solving the erosion process in comparison with implicit solver.

3.2 Governing Equations for Damage Initiation

The damage initiation criterion is a phenomenological way of predicting the onset of damage due to the impact of solid particles onto the target surface. This finite model assumes that the equivalent plastic strains at the onset of damage, ε_D^{-pl}, is a function of stress triaxiality and the strain rate [18]:

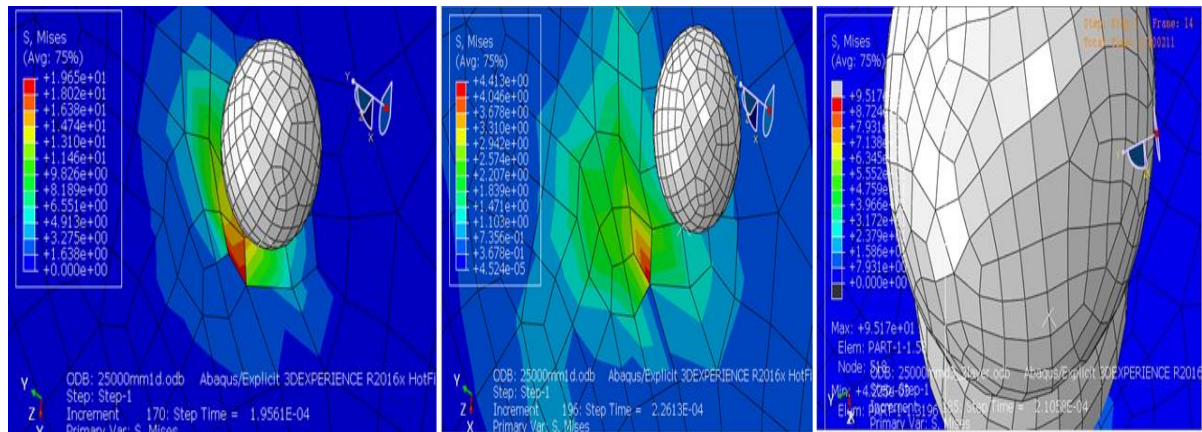$$\varepsilon_D^{-pl}(\eta, \varepsilon^{-pl})\dots\dots\dots\dots\dots\dots\dots\dots\dots\dots\dots\dots\dots (2)$$

Where $\eta = -p/q$ is the stress triaxiality, p is the pressure stress, q is the Mises equivalent stress, and ε^{-pl} is the equivalent plain strain rate.

The criterion for damage initiation is met when the following condition is satisfied.

$$WD = \int \frac{d\varepsilon-pl}{\varepsilon D-pl(\eta,\varepsilon-pl)}=1\dots\dots\dots\dots\dots\dots\dots\dots\dots\dots.(3)$$

where WD is a variable that increases monotonically with the plastic deformation of the target surface. At each increment during the erosion process, analysis of the incremental increase in WD is computed by:

$$\Delta W_D= \int d\varepsilon - pl/ \varepsilon_D^{-pl}(\eta, \varepsilon^{-pl}) \geq 0\dots\dots\dots\dots\dots.(4)$$

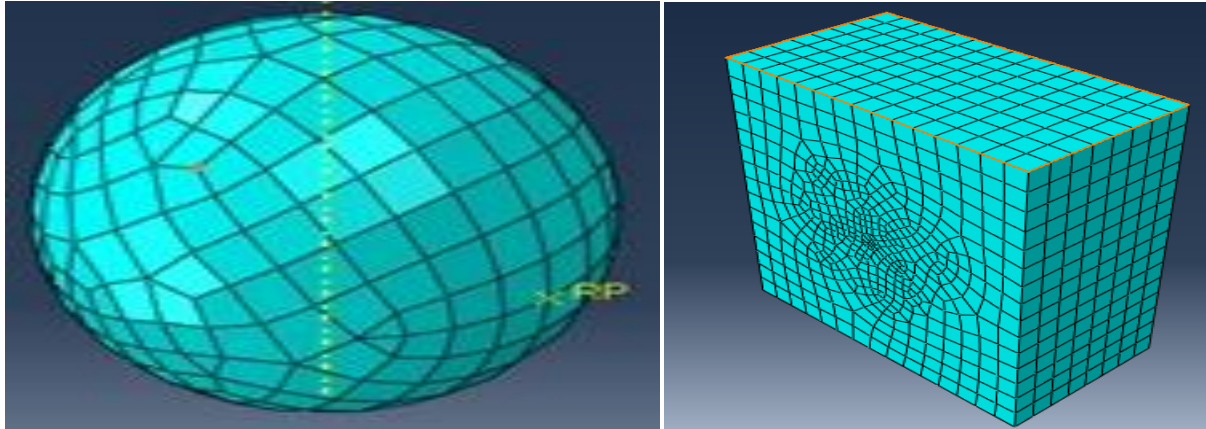Mithlesh Sharma, Deepak Kumar Goyal, Gagandeep Kaushal

Fig.- 4 Fringe diagram of Simulation results on substrate

3.3 General Contact Algorithm and Adaptive Meshing

Abaqus explicit provides the capability to choose general contact algorithm between the target surfaces and the erodent particles. General contact able the user to define the contact between two surfaces. In present investigation a Node based surface is used to model the eroding target surface. The erodent particles which are present in slurry are defined as Master surface and the target material surface are defined as slave surfaces. Penalty method is chosen for defining the contact which is based on coefficient of friction between two surfaces in contact with each other. The coulomb friction relationship has been used to define the contact between two surfaces which is defined in the equation below:

$$F = \mu R \ \dots\dots\dots\dots\dots\dots\dots\dots\dots\dots \ (5)$$

Where μ is the co-efficient of friction, R is normal force acting opposite to the weight of the body, and F is the frictional force acting opposite to the direction of motion of erodent particles. The coefficient of friction (l) based on the previous literature is taken as 0.3 between the target surface and the solid particles, which is valid for the contact between dissimilar materials used in this study. To co-relate the deforming behavior of target material in simulation, Adaptive meshing technique is used which gives capability to mesh to move independently on the damaged or deformed target material surface. This adaptive meshing technique provides Lagrangian and Eulerian analysis. Due to adaptive behavior of mesh, it alters the topology of mesh when there is large deformation or degradation on to the surface.

Research Cell: An International Journal of Engineering Sciences,

Special Issue November 2017(ETME-17), Vol. 25, Web Presence: http://ijoes.vidyapublications.com

ISSN: 2229-6913(Print), ISSN: 2320-0332(Online), UGC Approved Journal (S.No.63019)

© 2017 Vidya Publications. **Authors are responsible for any plagiarism issues.**

Fig.-5 Schematic representation of one of the solid particles used as erodent and substrate

3.4 Meshing Elements and Boundary Conditions

The substrate surface is coated with the powder of WC-10Co-4Cr having thickness of 250µm. substrate and coated surface are modeled as deformable rigid bodies with C3D8R meshing elements, which are 8-node linear brick elements. Erodent particles are considered as discrete rigid bodies R3D4 meshing elements, which are 4-node 3D bilinear rigid quadrilateral elements. The schematic view of the erodent particle and target surface which were taken in the study are shown in the figure 6. The target surface is having dimensions of 40 mm x 40 mm X 8 mm approximately and the erodent particle is drawn in spherical shape with diameter as 1 mm. The deposited surface coatings and substrate are considered together for modeling as shown in Fig. 5 b. The coated surface on which the impact of particles will be acted are constrained by imposing the boundary condition which constraint the target material from displacement and rotation in X, Y and Z directions. The representation of these constraints is shown in Figure 6. For defining the velocities of erodent's predefined field available in Abaqus is chosen and different velocity (25m/s,50m/s and 75m/s) for solid particles is defined for solid particles. Three velocities are taken for present study to correlate the simulation work with the experimental work. Erodent particles are defined only with respect to target surface. These particles are 3mm apart from each other.

4. NUMERICAL SIMULATION RESULTS AND DISCUSSIONS

### 4.1 Simulation Results for Surface Coatings

The simulations were carried out using four solid particles. The impingement angles for the erodent particle are taken as 90°. It has been observed that with the impact of first particle elements have failed which verify the fact that damage had taken place due to impact of initial particle. This damage was further propagated for succeeding impingement of the particles. This has been verified by observing the crater profile formed after the impact of the particle as shown in the figure. In light of the above simulation results, a thorough assessment and more simulations are carried out at the different impingement velocities of 25m/s, 50m/s and 75m/s. These simulation results show that the elements within the contact domain failed because of material damage/failure mechanism. The general contact considers the exposed faces only for the element failure and the underlying elements have not failed.

Mithlesh Sharma, Deepak Kumar Goyal, Gagandeep Kaushal
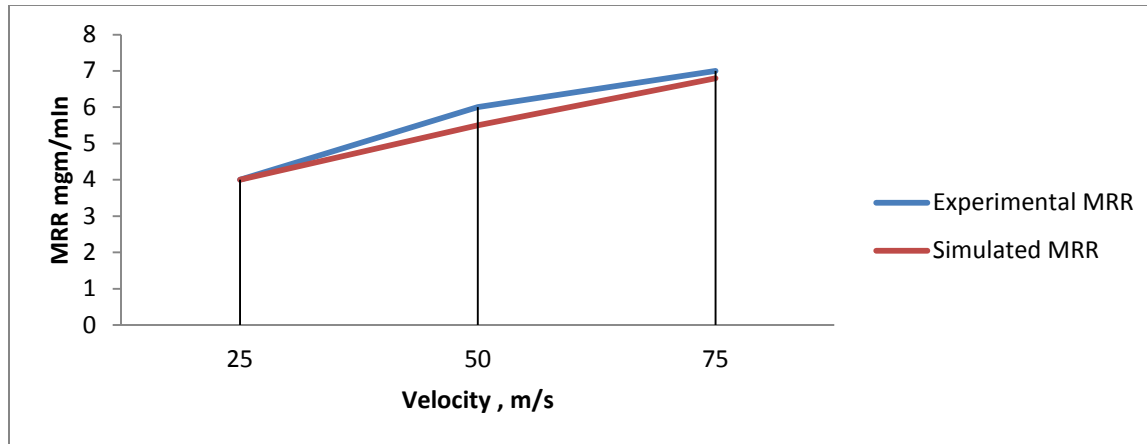
Fig.- 6MRR value obtained from FEA Simulation and Experimentation

Thus, the exterior faces of the elements are initially active and the interior faces are initially inactive. Once the exterior element fails, then its faces are removed from the contact domain and the exposed underlying exterior faces become active. This process is progressive for successive impingements. Hence, the general contact between the impinging particles and the target surface coating supports the idea of a damage/failure mechanism [18]. For 25m/s velocity it has been observed that crater area generated at impingement angle of 90° is somewhat lesser then the crater area formed by the impinging particles at impact velocity of 50m/s. It is due to the fact that at higher velocity, High kinetic energy is generated which resulted into higher thrust force which impacted the erodent particles into the coated surface. Similar phenomenon is observed while experimentation that higher mass removal will takes place at higher velocity. Similarly at higher velocity of 75m/s, more elements of the surface will failed which resulted into higher mass loss as comparison to other velocity. It has been also noticed that when consecutive particles are impinging on the surface of the target surface, particles are rebounded back and divert the coming erodent particle from its path which generate the same phenomenon as reported by the various researcher due to slurry erosion generally known as squeeze film effect. In figure graph has been shown between the stress and time it has been seen that when initially particle is striking on to the surface higher stress will generated and when it is propagated further, it started to decreases.
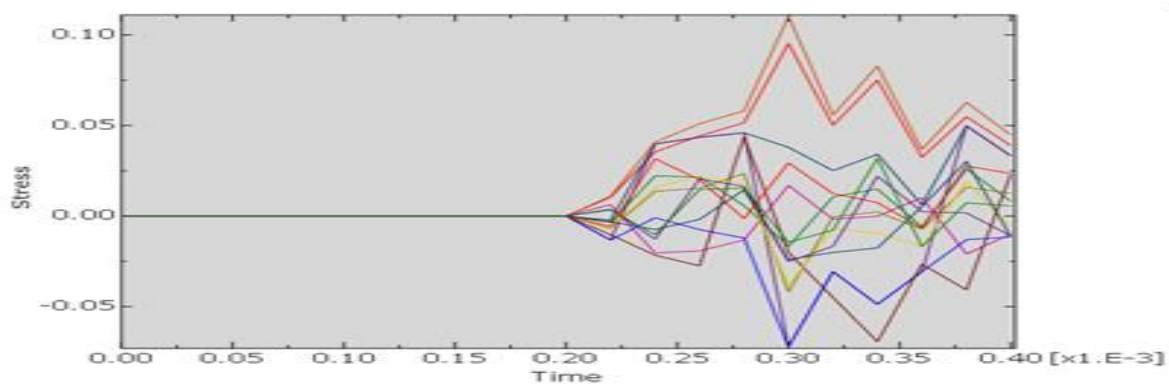
Fig.- 7 Graph Stress variation with respect to Time on a target surface

Mithlesh Sharma, Deepak Kumar Goyal, Gagandeep Kaushal
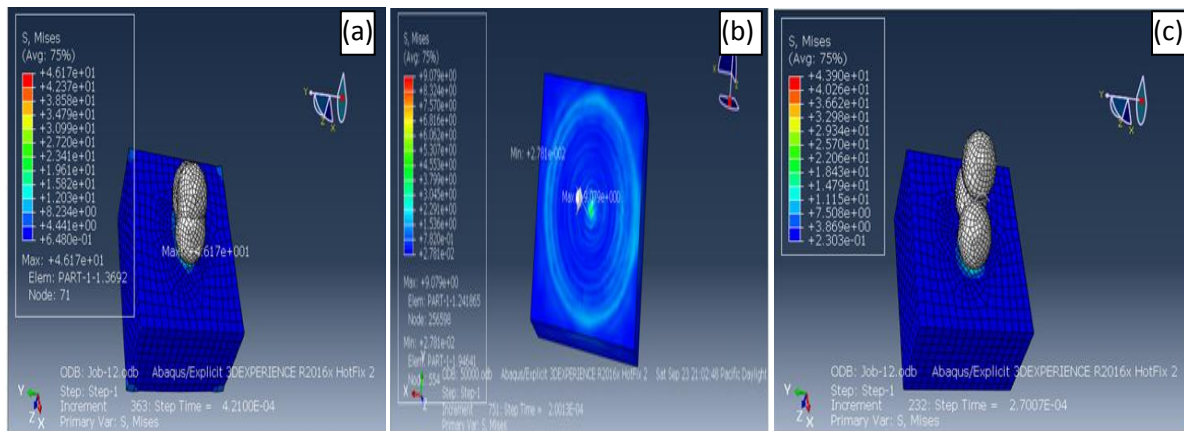
**Fig.- 8** Fringes of Mises stresses (a) 25m/s (b) 50m/s (c)75m/s

4.2 Material Removal Rates and Depth of Penetrations

In present study material removal rate is calculated with the help of numerical simulations. In numerical simulation material MRR is measured with the help of density and mass of the substrate along with coating. It has been found that initial mass of the target material was 153.450 grams. Layer of coating which was deposited on the substrate comprises 29,835 elements. Thus mass of each finite elements come to 0.0514 grams. The material rate is determined with the help of tool which is able to determine Number of failed elements in simulations. The MRR will be computed by multiplying the number of failed elements in given time with mass of each finite element. MRR obtained from simulation were compared with the results obtained by experimentation for 5mins time, as shown in Figure…. It was found that FEA based MRR values are in good agreement with the experimentally obtained results. The FEA calculated MRR values are in good agreement with the experimental values. The maximum depths of penetrations are calculated based on the distance from the damaged element to the undamaged element in the impingement area. The longitudinal cut of the damaged area, which is used for calculating the depth of penetrations, is shown in Fig. 11. The FEA-measured depths of penetration are shown in Fig. 12, and they are in good agreement with the experimental results.

4.3 SEM Characterization of Slurry Eroded Surfaces

To characterize the surface of the eroded section during experimentation SEM analysis was carried out. It was carried out to understand the erosion mechanism which had taken place on the surfaces. Figure 9 shows the typical SEM images of WC-10Co-4Cr steel damaged surfaces at different Velocities. These surfaces of the coating removal takes place as a result of the impact produced by the jet of slurry containing liquid and solid particles.SEM shown in the figure 9 revealed that different operating mechanism will be acting on the surface during impingement of the liquid. It has been observed that damage of the material takes place when the equivalent plastic strain value in the material exceeds the value of the failure.Damage in the surface occurred due to the consecutive impingements of the particles as a result of which micro cutting and material removal from the target surface takes place. This damage propagated due to successive impingements which causes micro cutting and material removal from the surface of the material.This damage on the surface occurred as a result of coincident cracks, fracturing of

fragments, pitting and crater formation. Figure 9 (a) shows the damage occurred at impingement velocity of 75m/s and shows the severely damaged surfaces, sub-surfaces and high depth of field. An increasing number of pits and a high degree of micro cutting of the material are present. Figure 9 (b) illustrates less carter formation in comparison with the crater formed at high velocity. Finally, the depth of field employed while viewing the samples in the SEM is directly proportional to the jet velocity used for a given sample, which supports the earlier penetration depth measurements from the ABAQUS/Explicit analysis and experimental results indicating that larger jet velocity create deeper erosion crater zones in the samples.
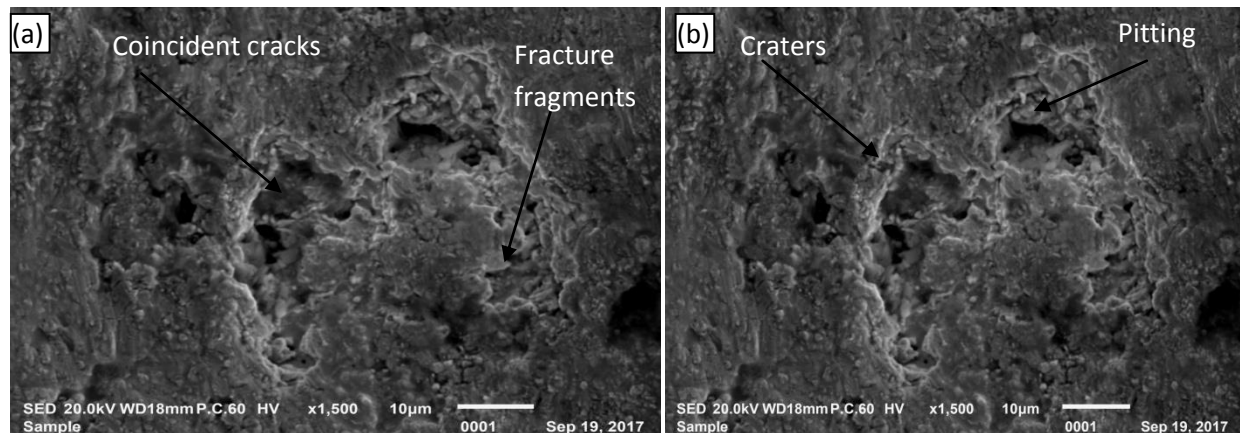
Fig. - 9 SEM images of WC-10Co-4Cr HVOF coated AISI304 Stainless steel

5. CONCLUSIONS AND FUTURE RECOMMENDATIONS

In this investigation a Material failure model was developed using three dimensional FEA software, Abaqus Explicit. In present numerical model Eulerian and Lagrangian approach has been used. In this model FEA concepts such as multiple particle impingement, element deletion and material failure model is used. Model presented in this investigation is able to predict the craters formation during the slurry erosion. It is able to tell us the amount of material deformed on the coating during the process. Result obtained using FEA Abaqus Explicit software were compared with the results obtained experimentally. It was found that results obtained were in line with those obtained experimentally. Along with result obtained, the location determined by the simulation results were in coincidence with experimental results.

The numerical simulation results verified the fact that extensive experimentation can be reduced with these simulation tests which will result in saving of time and money. These simulation models can be applied to various industries such as hydro power plant, mining, oil, marine, power generation industries etc. it was revealed that failure of material takes place when the strain induced in a material exceed the value of strain at failure. Eroded surfaces revealed micro cutting, pitting, micro cracks and coincident cracks were identified as a major mechanism which causes erosion of the surface.

REFERENCES

1. Goyal D K, Singh H, Kumar H and Sahni V, Journal of thermal spray technology, 21(2012),838-851.

2. Goyal D K, Singh H, Kumar H and Sahni V, Journal of Tribology, 136 (2014), 0416021-0416032.

3. Bajracharya T R, Joshi C B, Saini R P, Dahlhaug O G, Wear, 264 (2008),177–184.

4. Chawla V, Sidhu B S, Puri D and Singh P, Journal of the Australian Ceramic Society, 44 (2008), 56-62.

5. Bitter J G A, Wear, 6 (1) (1963), 5-21.

6. Prakash A, Srinivasan S M, Rao A R M, materials & design, 83 (2015) 164–175.

7. Nouraei H, Kowsari K., Samareh B., Spelt J K, papini m., journal of manufacturing processes, 23(2016), 90–101.

8. Perelstein Y N, Gutmark E, wear, 364-365 (2016), 169–183.

9. Qi H, Wen D, Yuan Qiao, Li Zhang, Zhenzhen Chen, powder technology xxx (2016) xxx–xxx.

10. Graham L J W, Wu J, Short G, Solnordal C B , Wong C Y, Brown G, Celliers O , Whyte D, hydrometallurgy, xxx (2016) xxx–xxx.

11. Peng W, Xuewen C, Powder Technology 294 (2016), 266–279.

12. Zhou Z Y, Yu A B. , Choi S K, powder technology 211 (2011), 237–249.

13. Zheng C, Liu Y , Wang H, Liu Z, Shen Y, Cai b, powder technology 303 (2016), 44–54.

14. Vieira R E., Mansouri A, Mclaury B S, Shirazi S A, powder technology 288 (2016), 339–353.

15. Mallmann F J K, Rheinheimer D D S, Ceretta C A, Cella C, Minella J P G, Guma R L, Povi V F, ecosystems and environment, 196 (2014), 59–68.

16. Graham L J W, Lester D and Wu J, seventh international conference on cfd in the minerals and process industriescsiro, melbourne, australia,9-11 december 2009.

17. Manjula E V P J, Ariyaratne W K H, Ratnayake C, Powder Technology, S0032-5910(2016), 30708-2.

18. Xu L, Zhang Q, Zheng J, Zhao Y, Powder Technology, 302 (2016), 236–246.

19. Wang M, Feng Y T, Pande G N, Chan A H C, Zuo W X, computers and Geotechnics, 82 (2017), 134–143

20. Kumara D, Bhingole P. P, "Materials Today, 2 (2015), 2314 – 2322.

21. Mansouri A, Arabnejad H, Karimi S, Shirazi S A., McLaury B S, Wear (2015), 339–350.

22. Chen J, Wang Y, Li X, He R Y,Han S, Chen Y, Powder Technology, 282 (2015), 25–31

23. Mansouri A, Arabnejad H, Shirazi S A, McLaury B S, Wear, 332-333(2015),1090–1097.

24. Arabnejada H, Shirazi S A, McLaury B S, Subramani H J, Rhyne L D, Wear, 332-333(2015),1098–1103.

25. Peters A, Sagar H, Lantermann U, Moctar O, Wear, 338-339(2015), 189–201.